Search Performance With PTN Successfully Predicts Search Performance With An Advanced Sensor

Melvin Friedman
Timothy C. Edwards
Max Lorenzo
Richard Vollmerhausen
Night Vision and Electronic Sensors Directorate
10221 Burbeck Road
Fort Belvoir, VA 22060-5806

ABSTRACT: In the experiments reported here, trained military observers first searched for tracked targets in approximately 100 synthetically generated Paint The Night (PTN) images. Months later, a different group of trained military observers searched for tracked targets using imagery obtained with a particular advanced sensor operating in the 8 - 12 μ band. In both experiments, the maximum amount of time t_L observers were permitted to search an image was controlled and took on the values 3, 6, 9 and 12 seconds. The probability P(t) for the observers detecting the target as a function of time was measured for different values of t_L, for targets that varied continuously between easy and hard to find, and excellent agreement in search performance was observed when comparing PTN and imagery obtained in field trials utilizing an advanced thermal imager. The excellent agreement in search performance using PTN and field imagery, the ability to control target signature and backgrounds in PTN and the relatively low cost of search experiments done utilizing PTN imagery, make PTN an excellent tool for search model development.

1.0 Introduction and Overview.

Search model development at NVESD is always validated with field experiments and up to this point has also been largely developed from field tests. Field tests are expensive, it is difficult to control target signatures, it is difficult to get a variety of targets and one must use sensors that are available. These issues are neatly dealt with by using synthetic Paint The Night (PTN) imagery.

However, using PTN raises a question: Can observer search performance measured using PTN imagery be used to predict how observers will do using real thermal sensors searching for real targets in the field? The chief purpose of this report is to answer this question. The methodology utilized in this report involves comparing search performance for observers viewing PTN imagery with performance for observers using imagery collected in the field using an advanced 8-12 μ sensor. Future work will investigate the suitability of PTN for search model development with other sensors.

All experiments involving search will result in the calculation of different parameter values for detection time and probability of detection for the imagery presented. This makes a direct comparison of the raw data impossible. The method chosen here to accomplish this comparison utilizes interpolation functions to exactly fit experimental data obtained from PTN imagery. Then the interpolation function PTN results are compared against real sensor data. This method was chosen instead of the typical model development methodology because the goal was not to develop a model, rather to compare results from one experiment to that of another. The notation utilized in this report is therefore, by necessity, different from that utilized in the classical search literature and will now be described.

We are interested in how observer search performance depends on the maximum amount of time t_L observers are permitted to search an image. In the experiments reported here observers are permitted to search for a maximum of 3, 6, 9, 12 and 17 seconds.

P_∞ is one of the parameters usually used to describe search. It is the fraction of observers viewing an image who correctly declare a target given a large value for t_L. The parameter P_∞ measures how difficult it is for an observer to find a target in an image. A problem with this parameter is that the value of t_L is not specified in the definition of P_∞. Conceptually, to get an accurate value for P_∞, t_L is infinite. However, as t_L increases beyond 15 or 20 seconds observers get bored and performance suffers. To measure P_∞ , a compromise is made between the conceptual requirement for a large value of t_L and the practical

necessity of keeping t_L small enough not to bore the observers. Historically, P_∞ has been measured with a t_L of about 30 seconds. In the research reported here, the issue of what t_L to use in measuring P_∞ is sidestepped by introducing a different parameter ... Pe12.

Pe12 is the fraction of observers viewing an image who correctly declare a target given a maximum search time of twelve seconds. It measures how difficult it is for an observer to find a target in an image. The "e" in Pe12 stands for *experimental.* Pm12 denotes the *modeled* valued for Pe12.

The form of the search model for the experiments reported here is:

$$P(t) = a\,(1 - e^{-\frac{t - t_d}{\tau}}) \qquad t_d \le t < t_L \tag{1.1}$$

In equation (1.1) t_d is the average time observers taking the experiment took to move the mouse pointer to the vicinity of the target and click. P(t) is the fraction of observers who declare a target in time t. In this report, t is the time from when the image is first presented to the time an observer clicks the mouse. Search research workers frequently use t to denote what in this report is denoted by $t - t_d$. Observe that equation (1.1) only applies for t between t_d and t_L. The parameter τ is a time constant which determines how quickly the function P(t) reaches its asymptotic value. It may seem strange that the symbol "a" is used instead of the usual symbol P_∞. The reason for this is that in equation (1.1) "a" is a function that depends on Pe12 and t_L. Similarly, τ and t_d are functions of Pe12 and t_L.

$$\begin{aligned} a &= a(Pe12, t_L) \\ \tau &= \tau(Pe12, t_L) \\ t_d &= t_d(Pe12, t_L) \end{aligned} \tag{1.2}$$

Equation (1.1) with "a", τ and t_d given by equation (1.2) accurately describe observer search performance for observers viewing PTN imagery (see Figure 3.1). Equations (1.1) and (1.2) imply that P(t) depends on t with Pe12 and t_L as parameters. **What is shown in this report is that functions a(Pe12, t_L), τ(Pe12, t_L) and t_d(Pe12, tL) can be determined using PTN imagery and then these same functions can be used in equation (1.1) to accurately (see Figure 4.1) predict search performance when observers view imagery collected with the advanced sensor.** Future studies will investigate how robust this result is for different sensors, targets, backgrounds and observers.

Although the functions a(Pe12, t_L), τ(Pe12, t_L) and t_d(Pe12, t_L) are expressed algebraically, the expressions are long. The reason is that the functions a(Pe12, t_L), τ(Pe12, t_L) and t_d(Pe12, t_L) are bilinear interpolating functions. Space limitations preclude exhibiting these functions here. More concise expressions could have been written by function fitting using the method of least squares, but these would not represent PTN search data as accurately as the bilinear interpolation functions. It should be realized that for the most accurate comparison between PTN and sensors, different "a" and τ and t_d functions are used for 1st and 2nd gen sensors.

2.0 Experimental Procedure.

2.1 Image Generation.

The first part of the experiment was done using computer generated PTN imagery; the second part of the experiment was done on field imagery obtained with an advanced thermal sensor.

Briefly, PTN imagery is computer rendered imagery of real topography with computer generated rocks, trees, bushes and roads. PTN has the capability to place realistic vehicle models anywhere in the imagery. The apparent background and target temperatures as well as observer position are computer inputs. This enables a computer-generated image to be made at any time in the diurnal cycle from any observer position. PTN renders Long Wave Infrared targets and backgrounds and calculates a transmission loss by applying Beer's law to each pixel in the scene based on pixel range and an input attenuation per kilometer parameter. Sensor effects are then applied in a post rendering process, either real-time or in non-real-time. A more complete description of how PTN imagery is generated is given elsewhere [1 – 3].

A description of the particular imagery used in the experiments follows. Targetless, high resolution imagery, with trees, rocks, topography and roads typical of what is found at a U.S. Army site was generated for a particular region viewed from several positions on the perimeter of the region. Topography at the army site was sampled with an eight meter Cartesian grid before computer rendering. In each case the sensor was approximately five feet above ground level yet could see for a considerable distance because the sensor was located on the side of a hill. Nominally, one hundred high-resolution, pristine images were generated for several regions. Each PTN image had a field of view of 5.4 by 4 degrees, intermediate between that of a typical 1st and 2nd gen sensor.

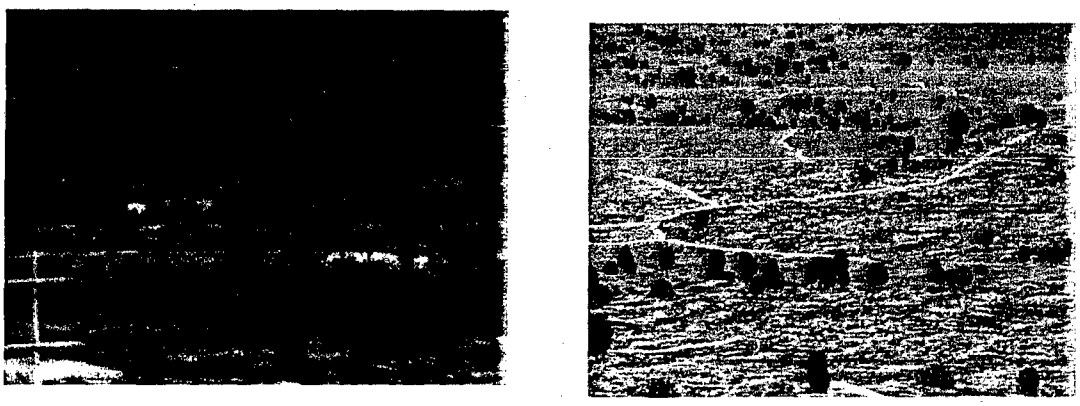

Figure 2.1. A representative advanced sensor image characterized by Pe12 ≅ 0.5 is shown on the left. Shown on the right is the corresponding second gen PTN image. Although a skilled observer has no trouble distinguishing an advanced sensor image from a PTN image, the PTN image is useful for preliminary search model development. The actual imagery seen by observers on monitors is better than that shown in this reproduction.

A single high-resolution target, selected from a set of targets was inserted into 68 of the images at realistic positions. The class of targets includes: M1A1, M60A3, HMMWV-Tow, BMP1 and an M113. Allowed target aspect angles include views at 0°, 30°, 150°, 270° and 330°. Aspect is defined as vehicle orientation relative to the sensor. Zero degrees correspond to looking at the target head on, ninety degrees corresponds to a direct view of the left side of the target and 270° corresponds to a direct view of the right side of the target.

The point spread function of 2nd gen imagery was generated by convolving: 1) the diffraction point spread function of a typical 2nd gen lens, 2) a Gaussian aberration blur function of a typical 2nd gen lens and 3) the spatial rectangle function associated with the finite size of a typical 2nd gen detector.

The PTN imagery was spatially sampled at a rate three times higher than the respective sensor resolution.

Each of the 100 images was convolved with point spread functions typical of a 2nd gen sensors as described above. No noise was added to the 2nd gen imagery. The 2nd gen imagery was DC coupled.

A goal in creating the PTN imagery was to have a range of easy and difficult targets so that the detection probability was uniform for 2nd gen sensors. This was accomplished by suitably adjusting target range, target signature strength and background signal strength.

Figure 2.1 compares a typical advanced sensor image with a simulated 2nd gen PTN image used in the perception experiments.

2.2 Power Point Presentation.

Observers viewed the PTN and advanced sensor imagery on individual monitors in groups of about seven over a period of several months. The number of observers who could take the perception test had to be seven or less because of the difficulty in fielding more than seven computers. To assure that observers received identical instructions in all sessions, instructions were given to the observers in a power point presentation.

A summary of these instructions follows. The observers were told a scene may or may not have a military vehicle in it. If a vehicle is present the observer's job is to find it; otherwise they were required to decide no vehicle is present as quickly and accurately as possible. Observers were shown a single image with five targets at five aspect angles displayed in a 5 x 5 matrix. They were then shown examples of representative targets seen with simulated 2nd gen imagery at different times of day, at different ranges and with different clutter.

Observers were also instructed in the mechanics of taking the test by the Power Point presentation. In particular, observers were shown the outline of a square that would move with the mouse and were told they would get credit for a correct detection if any part of the square overlapped any part of the target. This technique enabled the observers to quickly communicate perceived target location and is important in an experiment designed to measure detection time. Observers controlled when the next image was presented by pressing the space bar. When a new image appears, the square controlled by the cursor is automatically positioned at the center of the image. Observers were told this was a timed test and were encouraged to work as quickly as possible.

Definition of Detection. Observers were told if they saw something that they were uncertain about, but for which they would normally switch to a higher magnification, they should click on the object. If there are several items that satisfy this criterion, the observers were instructed to click on the one they thought was most likely to be the target. This defines detection for this test. This definition represents a change from the definition of detection [4] used previously at NVESD.

Definition of No Target Present. If the observer did not see a target and saw no object that they would examine more closely at higher magnification, then they were instructed to click the "No Target Present" button.

There was a practice session before taking the test and observers could practice as long as desired. They were also given a chance to ask the test administrator questions before taking the test.

2.3 The Experiment.

The observers were trained military personnel who were exceedingly good at finding targets. For some images, trained military observers could detect the target even when the authors of this paper had trouble seeing the target when cued to target location. The ability, displayed in this experiment, of the trained military observers to detect targets is awesome.

The experiment consisted of several sessions spaced nominally one month apart. This allowed us to determine that the experiment was well designed before having many observers take the test.

In the experiment, the observers could effectively make three choices: 1) if they thought they found the target, they could use a mouse to position a square box on the target and then click; 2) if they believed no target was present in the image they could click on a no target present box; 3) if they exceeded the time allowed to communicate a response, the current image would disappear. An observer caused the next image to be displayed by pressing a space bar.

The observers were given 3, 6, 9, 12 and 17 seconds to look at the imagery. They were also given as much time as they wanted to look at the imagery. Observers rarely needed more than 17 seconds to make a targeting decision. In those few cases where this occurred, it is believed this is due to an attention lapse. In a practical sense, 17 seconds corresponds to giving the observers as much time as they could productively use to find the target. The 100 images were shown to each observer in a random order without repeats i.e. like showing each card in shuffled deck. Each time the 100 images were shown, they were shown in random order. To assure the observers did not memorize the imagery, observers were shown the imagery first for 3 seconds, then for 6 seconds, then for 9, 12 and 17 seconds. In the final stage of the experiment observers could study the imagery as long as desired. Here we only report the data for 3, 6, 9 and 12 seconds. The reason: when observers were given more than 12 seconds they were fatigued. This compromised the credibility of data taken after 12 seconds.

Each observer took the experiment independently. A personnel computer was assigned to each observer for the duration of the experiment. The experiment took place in one dimly lit room.

PTN search sessions were done over the first three months. Advanced sensor sessions were done in the second three months.

2.4 Computer Hardware and Software.

The time to record a search choice depends on the quality of the mouse. For that reason, each observer was equipped with a recently purchased mouse and each mouse was tested to assure it was in excellent operating condition before it was used in the experiment.

Observers communicated with the computer by using the mouse to move a pointer and then clicking. When the pointer was on the image it assumed the shape of a square box with a 2 pixel wide line measuring thirty-six pixels on each side. This yields an area equal to approximately 1/300 the picture area. Observers indicated they found a target by positioning this square so that it overlapped any portion of the target. We were interested in how long it took the observers to find the target and did not want observers to spend an inordinate amount of time positioning the square on the target. For this reason, events where the observer clicked the mouse when any part of the square overlapped any part of the target count as correct. The observers were told this and they were urged to work as quickly and accurately as they could in a Power Point presentation before the test. When an observer believed no target was present, the mouse was moved to the side of the image where the pointer changed from a square to an arrow and the observer clicked a "No Target Present" button. If time ran out before the observer could communicate a decision, then a "Time Out" was recorded. The observer pressed the space bar to display the next image.

To get accurate detection times, mouse clicks are automatically recorded with the clock internal to the computer. Recently purchased personal computers and skillful programming assure these factors contribute a negligible error in the measured time it took an observer to make a decision.

3.0 Data Analysis.

To start with there are 100 PTN images and 100 advanced sensor images. In principal, each PTN image and each advanced sensor image could be individually analyzed but if that were done, with approximately 30 observers, the statistical error inherent in the search process dominates the results. For this reason, PTN and advanced sensor images were binned into four groups according to how difficult it is to acquire the target. The four PTN groups had Pe12 values of: 0.857, 0.560, 0.423 and 0.230. The four advanced sensor images had Pe12 values of: 0.86, 0.63, 0.47 and 0.32. Because the Pe12 values for PTN images are not identical to the Pe12 values for the advanced sensor images, P(t) values obtained using PTN imagery can not be directly compared with P(t) values obtained using advanced sensor imagery.

For a group of PTN images characterized by a particular Pe12 and t_L values, "a", τ and t_d values were determined by doing a least square fit to the experimentally determined P(t) vs t data. The Mathematica, Nonlinear Regress program that utilized the Levenberg-Marquardt algorithm, was used.

At this point we have tables of "a", τ and t_d as functions of Pe12 and t_L. One approach is to determine the equations (1.2) by assuming a functional form for these equations and then do a least squares fit. This approach was tried and was not completely satisfactory because it is difficult to know what functional form to assume. For the functional forms we assumed, the fit function matched the experimentally determined values of "a", τ and t_d with accuracies of about 10 %. However when these values where used in equation (1.1) the mathematical description of the experimental results was frequently off by 15 to 25 %. We were not satisfied with the accuracy with which the least squares approach described PTN experimental data and this caused us to consider a different approach.

Bilinear interpolation is the alternate approach. Abramowitz and Stegun [5] give the algorithm used. Bilinear interpolation reproduces the table of "a", τ and t_d as functions of Pe12 and t_L exactly and gives reasonable interpolations for these functions for Pe12 or t_L values that are not in the table. As illustrated in Figure 3.1, PTN search data was described mathematically by equations (1.1) and (1.2) with a high degree of accuracy. As illustrated in Figure 4.1, bilinear interpolation with parameters determined from PTN search experiments allowed accurate predictions of field search performance with an advanced sensor.

A graphical description of the functions $a(Pe12, t_L)$, $\tau(Pe12, t_L)$ and $t_d(Pe12, t_L)$ is exhibited in Appendix A. A description of the bilinear interpolation method and its virtues for the work described here is given in Appendix B.

4.0 Results.

Figure 4.1 shows a comparison of the mathematical model derived from PTN imagery and observer response to field imagery obtained with an advanced sensor. The agreement between the mathematical model and field imagery supports the view that PTN is an excellent tool for search model development.

5.0 Conclusions.

Equations (1.1) and (1.2) accurately represent search results when observers view PTN imagery and when observers view field imagery obtained with an advanced sensor (see Figures 3.1 and 4.1).

Measurements of observer response to PTN imagery allow accurate search predictions to be made for observers using an advanced thermal sensor (see Figure 4.1). Future studies will investigate how robust this result is for different sensors, targets, backgrounds and observers.

This investigation supports the view that PTN is a highly cost effective and useful tool for search model development. Of course a model developed from PTN imagery needs to be verified and validated with search experiments done on imagery collected in field tests.

Bilinear interpolation functions accurately summarized observer search response to PTN images (see Figure 3.1). This technique, rarely used in search modeling, was useful and is expected to gain wider use.

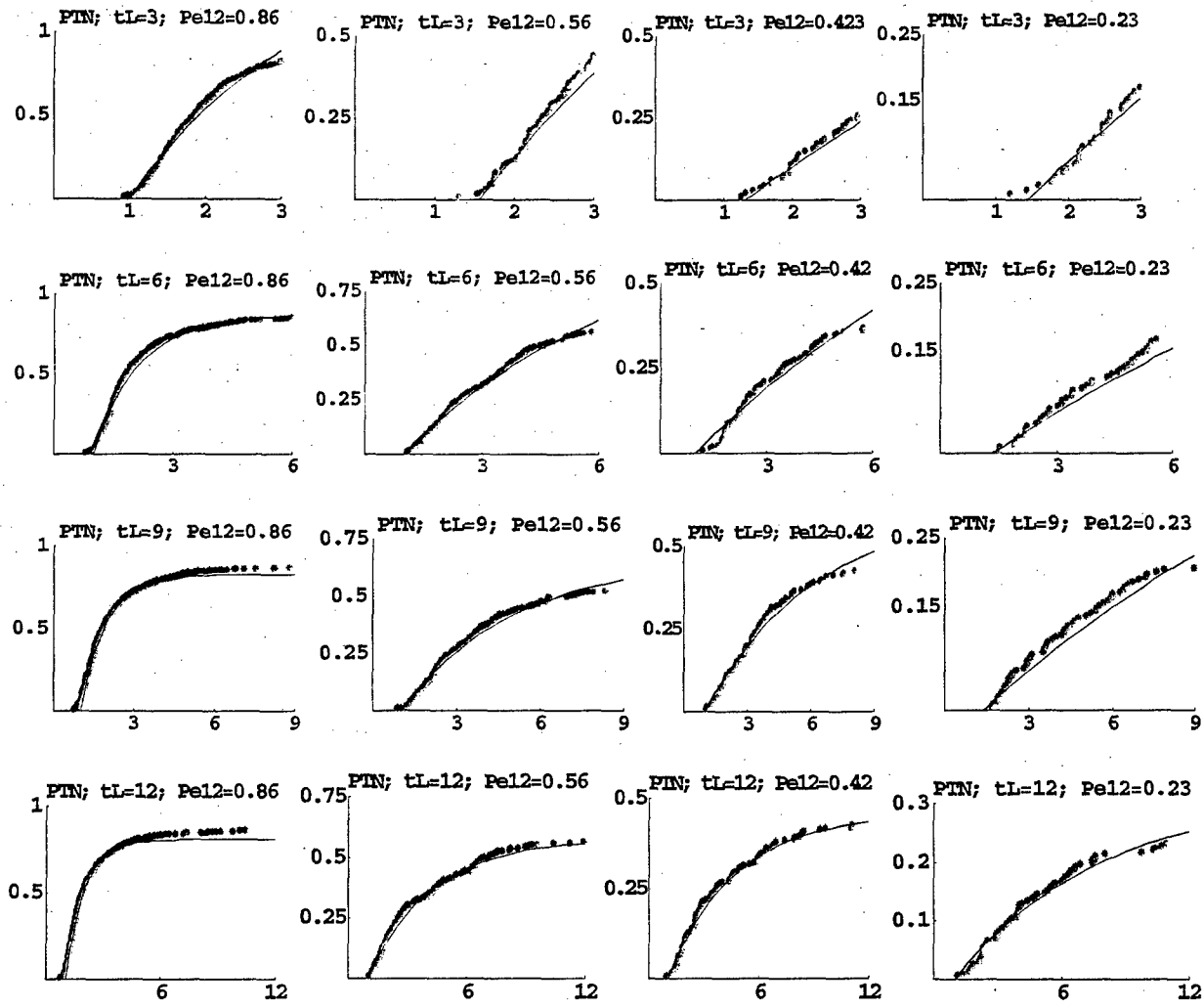

Figure 3.1. Shown above are graphs comparing a mathematical model, derived from observer response to PTN imagery, with the actual response of observers viewing PTN imagery. In each graph the horizontal axis corresponds to time and the vertical axis to probability of detection. The solid lines represent the results of the mathematical model and the dots represent observer response. As one goes from graph to graph, the probability of the observers detecting a target Pe12 changes in the horizontal direction; the maximum amount of time t_L observers are permitted to search an image changes in the vertical direction. The close agreement between the mathematical model and observer response demonstrates how well equations (1.1) and (1.2) describe observer response to PTN imagery.

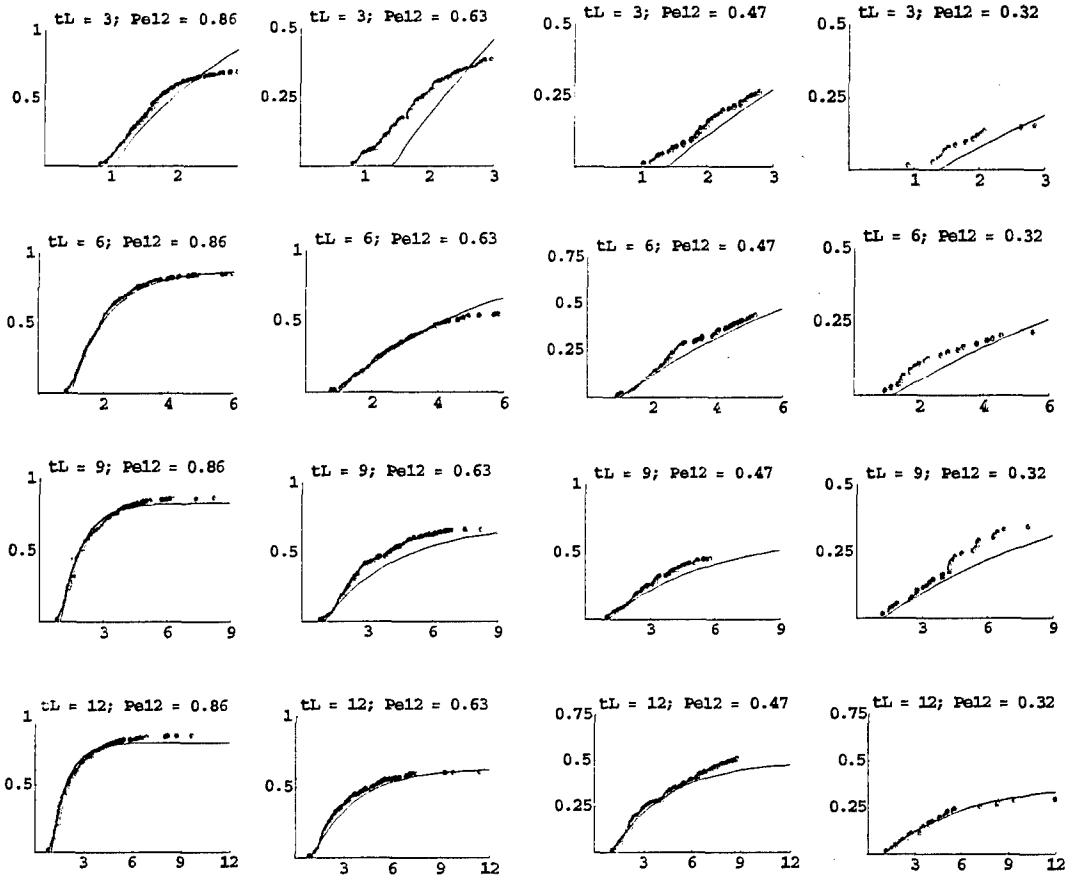

Figure 4.1. Shown are graphs of a mathematical model, derived from observer response to PTN imagery, with the response of observers using an advanced thermal sensor and real targets. In each graph the horizontal axis corresponds to time and the vertical axis to probability of detection. The solid lines represent the mathematical model and the dots represent observer response using an advanced imager. As one goes from graph to graph, the probability of the observers detecting a target Pe12 changes in the horizontal direction; the maximum amount of time t_L observers are permitted to search an image changes in the vertical direction. The agreement between the mathematical model and observer response using the advanced sensor is remarkable. The agreement between the mathematical model and field imagery supports the view that PTN is an excellent tool for search model development.

Appendix A. Graphical Representation of the Functions a(Pe12, t_L), τ(Pe12,t_L) and t_d(Pe12,t_L)

Using the bilinear interpolation method described in Appendix B, the functions a(Pe12, t_L), τ(Pe12, t_L) and t_d(Pe12, t_L) were determined from observer search response to PTN images using methodology described in section 3. Figure A.1 shows these functions graphically.

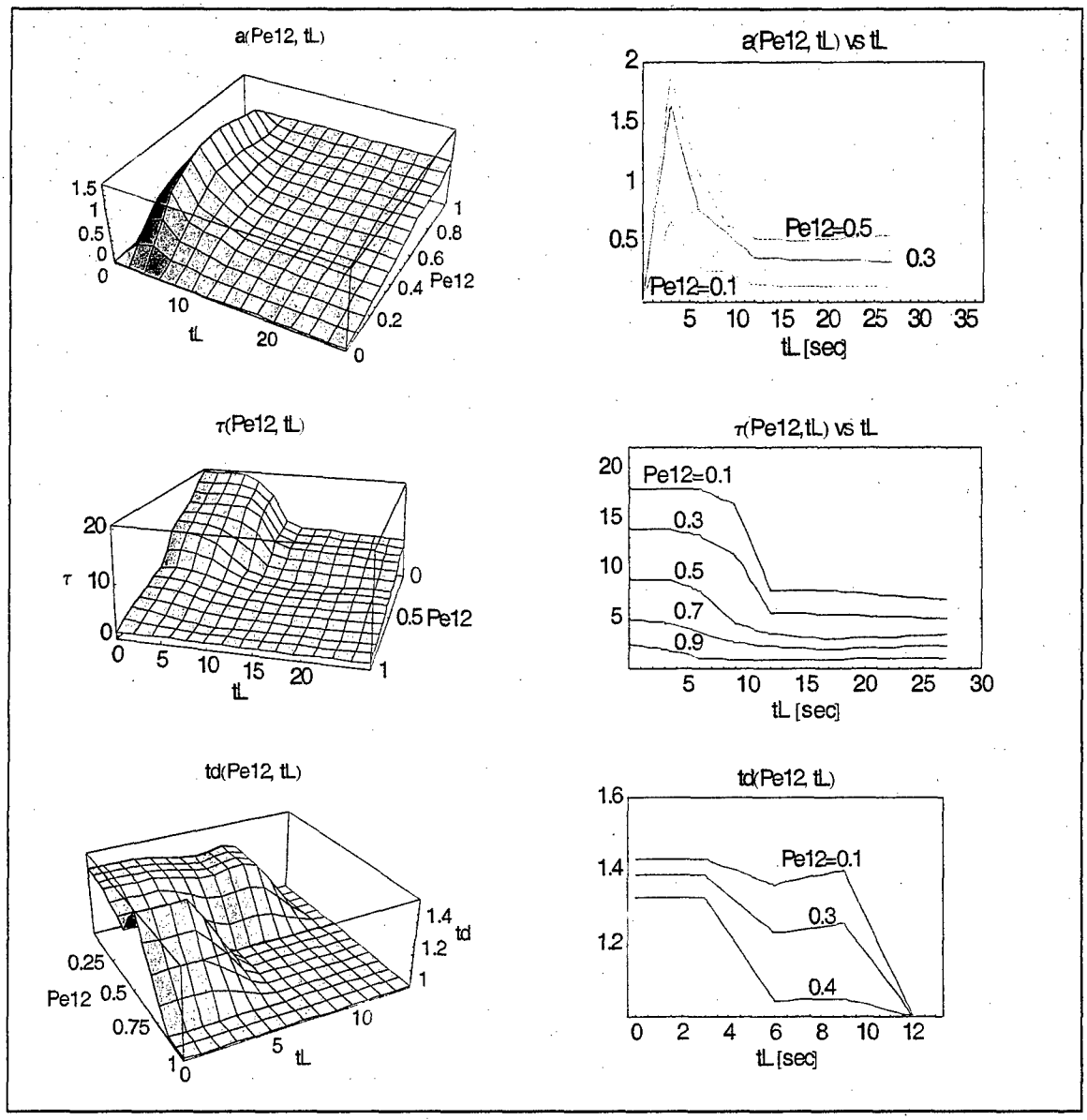

Figure A.1. Surfaces depicting a(Pe12, t_L), τ(Pe12, t_L) and t_d(Pe12, t_L) determined from observers viewing PTN images are shown on the left. Parametric curves for those surfaces are shown on the right.

Appendix B. Bilinear Interpolation and Its Virtues

The caption to Figure B.1 defines the problem which bilinear interpolation solves.

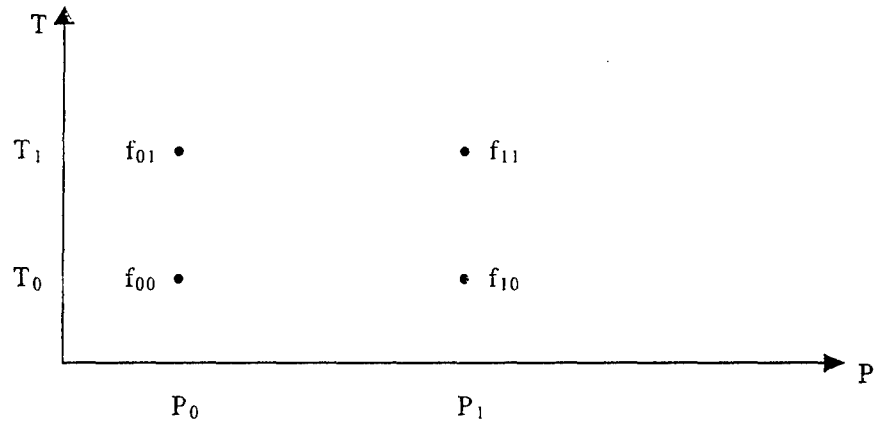

Figure B.1. In this figure P is an abbreviation for Pe12 and T is an abbreviation for t_L .The symbol f can be either "a", τ or t_d. With f_{00}, f_{10}, f_{01} and f_{11} known, the objective of bilinear interpolation is to estimate f when P is between P_0 and P_1 and T is between T_0 and T_1.

Define reduced variables p and t:

$$p \equiv \frac{P - P_0}{P_1 - P_0}$$
$$t \equiv \frac{T - T_0}{T_1 - T_0} \qquad \text{(B.1)}$$

Observe in equation (B.1) that as P varies between P_0 and P_1, p varies between zero and one. Similarly as T varies between T_0 and T_1, t varies between zero and one. The bilinear interpolation function f(P, T) is:

$$f(P,T) = (1-p)(1-t)\,f_{00} + (1-p)\,t\,f_{01} + p(1-t)\,f_{10} + p\,t\,f_{11} \qquad \text{(B.2)}$$

The interpolating function (B.2) has desirable properties.

- f matches the data points exactly.
  - When p and t are zero, $f = f_{00}$
  - When p and t are one, $f = f_{11}$
  - When p equals one and t equals zero, $f = f_{10}$
  - When p equals zero and t equals one, $f = f_{01}$
- The center point averages the surrounding points.
  - When p equals ½ and t equals ½ , $f = ¼ (f_{00} + f_{10} + f_{01} + f_{11})$
- f is linear in p and in t.
  - This implies that if t is held constant, f interpolates linearly between data points with different p. Similarly if p is held constant, f interpolates linearly between data points with different t.
- The preceeding bullet implies the interpolating function produces a continuous surface.
  - This is important because a small change in p or t should not cause a discontinuous change in the probability for detecting the target.

REFERENCES

1. Lorenzo, M., Jacobs, E., Moulton, J.R., Jr., "Optimal Mapping of Radiometric Quantities in OpenGL," Proceedings of SPIE, April 1999.
2. Lorenzo, M., Moulton, J.R., Jr, "Fidelity Requirements for EO Sensor Simulations" Proceedings of the Spring 1997 Simulation Interoperability Workshop, March 1997
3. Lorenzo, M and Moulton, R. "Toward Standards for Interoperability and Reuse in IR Simulation", Proceedings of the Fall 1997 Simulation Interoperability Workshop, September 1997.
4. The standard definition of detection used at NVESD: A target is said to be detected when a trained military observer can determine with some confidence that the object is of military significance. See M. Friedman et al. "Standard Night Vision Thermal Modeling Parameters", Infrared Imaging Systems: Design, Analysis, Modeling, and Testing III, p 204, SPIE Proceedings, Vol 1689 (April 1992).
5. Handbook of Mathematical Functions With Formulas, Graphs and Mathematical Tables, Editors M. Abramowitz, L. A Stegun, National Bureau of Standards Applied Mathematics Series 55 (1964). See equation 25.2.66.